Journal of Ovonic Research Vol. 5, No. 4, August 2009, p. 117 - 127

DC CONDUCTIVITY AND OPTICAL PROPERTIES OF $InSbTe_3$ AMORPHOUS THIN FILMS

E. Abd El-Wahabb, A.E. Bekheet, A.H. Ashor* ,H.E. Atyia and M.A.Afifi
Physics Department, Faculty of Education, Ain Shams University, Roxy, Cairo, Egypt.
**National Center for Radiation Research and Technology.*

Measurements of dc electrical conductivity and optical properties have been made on $InSbTe_3$ thin films prepared by thermal evaporation having different thickness (25-150) nm range. The structure of $InSbTe_3$ in its powder and thin film forms were investigated by X-ray diffraction (XRD). The electrical conductivity was measured in the temperature (303-392) K range. The obtained values of dc electrical conduction activation energy ΔE_σ were found to be nearly independent on the film thickness and have the mean value of 0.173 eV in the range considered. The refractive index *n* and the absorption index *k* were determined in the spectral range 400-2500 nm. It is observed that *n* decreases with increasing film thickness at any wave length, while *k* is practically independent on film thickness in the range 25-150 nm. For films with thicknesses in the range 170-304 nm, the spectral distribution of transmittance T and reflectance R showed that T+R<1 in the whole spectrum which due to light scattering by surface roughness whose existence is confirmed by electron microscopy. Analysis of *k* indicated that the absorption mechanism refers to the existence of indirect transitions with an optical energy gap of 0.52 eV.

(Received August 10, 2009; Accepted August 20, 2009)

Keywords: DC conductivity, $InSbTe_3$, Amorphous, Thin film

1. Introduction

In_2Te_3 is a semiconductor material with a defect crystal structure which is of the sphalerite type and contains 5x 10^{-3} /cc empty neutral sites in the cation sublattice [1]. It has two phases (α and β) [2, 3]. Many physical properties of In_2Te_3 were investigated earlier by several authors [1, 4-7]. In_2Te_3 and its solid solutions have valuable photoelectrical properties, low sensitivity to impurities and low thermal conductivity.

Sb_2Te_3 has narrow energy gap corresponding to weak polarity of bonds between Sb and Te. It is a low- resistively chalcogenide, whose solid solutions have good thermoelectric properties in the range (200-600K). Several authors investigated its electrical and optical properties [8-10].

The In_2Te_3 – Sb_2Te_3 system ($Sb_{2-x}In_xTe_3$ solid solution) belongs to the family of layered compounds having the structure of space group D_{34}^5. Physical properties of single crystals of $Sb_{2-x-}In_xTe_3$ compounds were described in a number of papers [11-15]. However, little attention was devoted to study physical properties for $InSbTe_3$ thin films [16-17].

This paper aimed to investigate the structure, electrical and optical properties of $InSbTe_3$ amorphous thin films with different thicknesses.

2. Experimental procedure

$InSbTe_3$ compound was prepared in a bulk form by direct fusion of the 99.999 purity constituent elements In, Sb and Te. The components were mixed inside a sealed evacuated silica tube (10^{-5} Pa) and melted using a constructed oscillatory furnace, which ensure the homogeneity of the composition. The furnace temperature was raised to 1003 K at a rate of $50Kh^{-1}$ [18] and kept constant for 48 hours. Then, the temperature of the furnace was decreased at a rate of 3 K min^{-1} to room temperature.

$InSbTe_3$ thin films of different thickness were prepared by thermal evaporation on dry-clean glass substrates under vacuum of 10^{-5} Pa using a coating unit (Edward 306 A). The film thickness was measured by Tolansky's interferometric method.

The structure of the investigated composition in powder and thin film forms was investigated by X-ray diffraction analysis by using a Philips X-ray diffractometer with Cu target and Ni filter operated at 36 kV and 20 mA to give X-rays with wavelength 1.542 A^o. The chemical composition was checked by energy dispersive X-ray analysis (EDX) using a scanning electron microscope (Joel 5400).

Dc conductivity was measured for thin films of different thicknesses, sandwiched between two Al electrodes. Their resistance R was measured using a digital electrometer (Keithley type E616A). The conductivity was calculated by the relation

$$\sigma_{dc} = \left(\frac{d}{A}\right)\frac{1}{R}, \qquad (1)$$

where d and A are the thickness and the cross-sectional area of the film respectively.

The optical properties of the as deposited thin films of different thicknesses were investigated. The transmission, T, and reflectance, R, of each film were measured at room temperature using a dual beam spectrophotometer (JASCO Corp.V-750, Rev.1.00.) equipped with unpolarized light at normal incidence in the spectral range from 500 nm to 2500 nm. Optical microscope photographs were made using optical microscope (Kyowo Tokyo No.873234 with magnification 1200) to clarify the nature of the film' surface.

3. Results and discussion

3.1 Structural identification

EDX analysis indicated that the composition of the prepared material as powder and thin film forms are $In_{19.7}Sb_{17.3}Te_{63}$ and $In_{23.1}Sb_{18.81}Te_{58.09}$ respectively. This is close to $InSbTe_3$, with an experimental error of ±2%.

X-ray diffraction patterns for $InSbTe_3$ as powder form is given in Fig.1(a). This figure illustrate that the powder form has polycrystalline structures. In addition, by comparing the measured XRD pattern with the XRD patterns of In_2Te_3 and Sb_2Te_3 binary compounds and pure constituent elements, no line matching is observed. The absence of the lines of binary compounds and pure constituent elements in the measured pattern shown in Fig.1(a) indicates the formation of $InSbTe_3$ ternary composition. Fig.1(b) shows the XRD patterns of $InSbTe_3$ thin films having different thicknesses in the (25-304) nm range. It is observed that all thin films in this range have an amorphous structure.

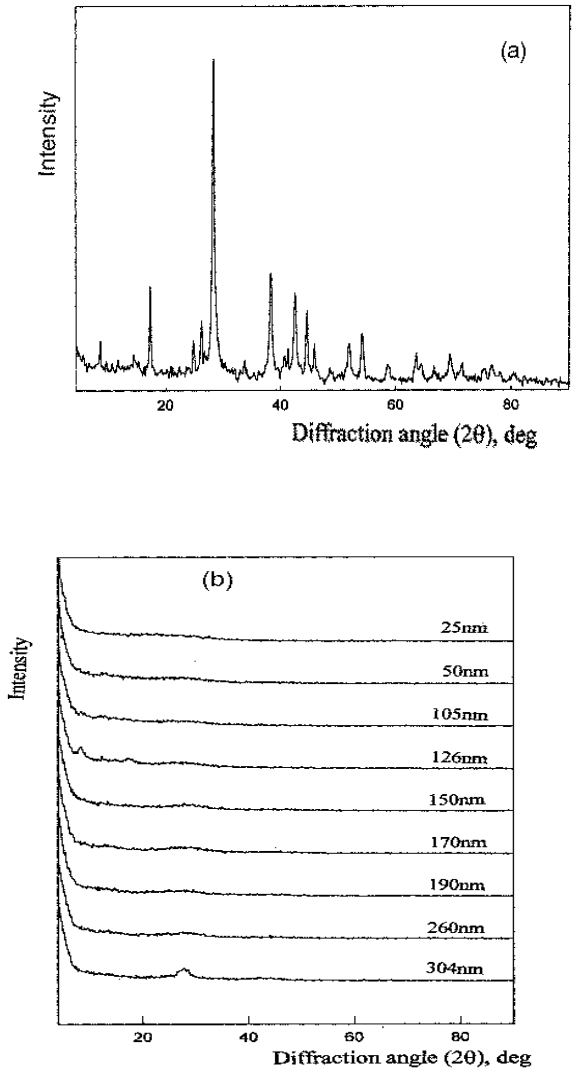

Fig. 1.a-X-ray diffraction patterns of $InSbTe_3$ in powder form
b-X-ray diffraction patterns of $InSbTe_3$ for thin films of different thicknesses .

3.2 Dc electrical conductivity of $InSbTe_3$ thin films

3.2.1 Thickness dependence of electrical conductivity

The room temperature dc electrical conductivity σ_{dc} for the as-deposited $InSbTe_3$ thin films of (50-150) nm thickness range was measured. The results are shown in Fig.2. It is clear from this figure that σ_{dc} increases with increasing film thickness. This behaviour can be attributed to lattice defects, such as vacancies, interstitials and dislocations which might be distributed through the first stages of the film growth. These defects add extra percentages of resistivity. As the film thickness increases, these defects diffuse and the corresponding resistivity decreases, hence the conductivity increases with film thickness. The obtained room temperature dc electrical conductivity of the investigated films of the order of $10^{-6}\ \Omega^{-1}\ m^{-1}$ is higher than that for In_2Te_3 thin films with the same thickness ($\sim 10^{-7}\ \Omega^{-1}m^{-1}$)[6]. This is because the increase of Sb atoms increases the free carrier concentration [14, 19] and hence increases the conductivity.

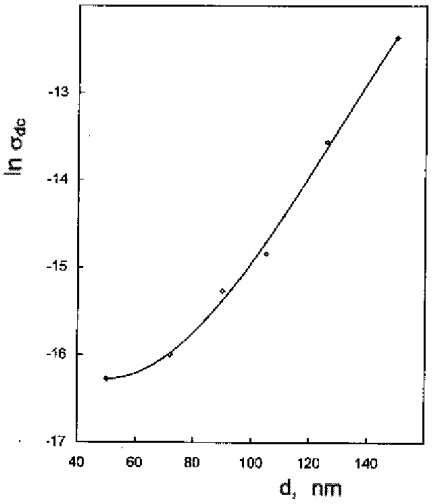

Fig.2. Thickness dependence of room temperature dc conductivity σ_{dc} for $InSbTe_3$.

3.2.2 Temperature dependence of electrical conductivity

The temperature dependence of electrical conductivity (σ_{dc}) was studied in the temperature range (303-393 K) for the as-deposited films of the thickness (50-150) nm range. The obtained results illustrated in Fig.3, from which it is shown that the conductivity increases with increasing temperature. This behaviour indicating the presence of semiconducting properties of the $InSbTe_3$ thin films as that reported for other compounds [20] and may be due to the kinetic of the film growth and diminishing the density of structural defects [21]. The mean value of the activation energy of (0.173 eV) is calculated from the slopes obtained from the linear fit of measured data shown in Fig.3 that also shows a set of nearly parallel straight lines, using the relation.

$$\sigma = \sigma_o \exp(-\frac{E_\sigma}{KT}), \tag{2}$$

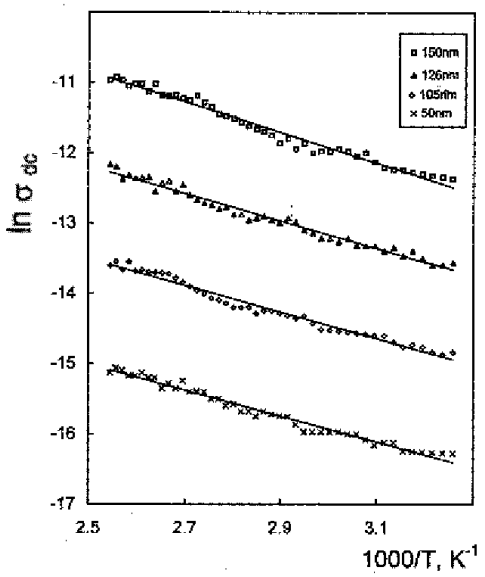

Fig.3. Temperature dependence of dc conductivity σ_{dc} for $InSbTe_3$ thin films of different thicknesses.

where σ_o is the pre-exponential factor, K is Boltzmann constant and T is the absolute temperature. According to the Davis and Mott model [22] for the density of states of amorphous semiconductors, the value of the activation energy is expected to be smaller than half the optical energy gap by the width of the localized states E_e. Since E_g^{opt}=0.52 eV and E_e= 0.059 eV as obtained below, so the expected value of the activation energy is ~ 0.201 eV. The difference between the expected and the obtained mean value can be explained by a shift in Fermi level due to the inequality of positive and negative charge dangling bonds, observed in chalcogenide glasses [23, 24].

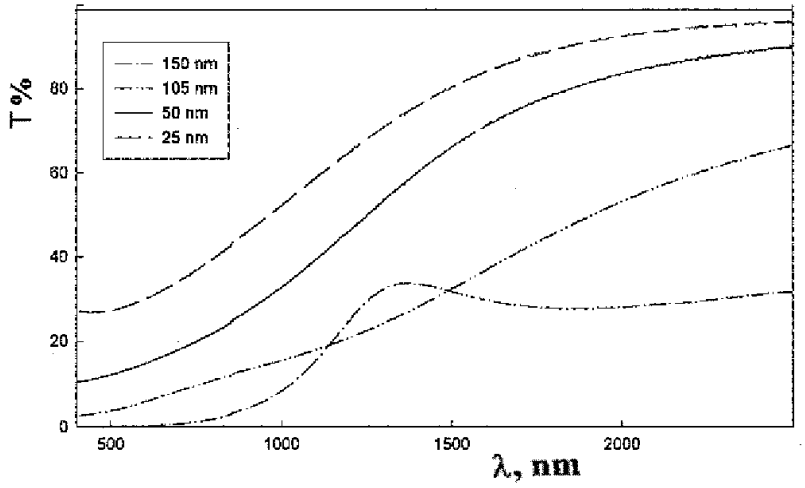

a

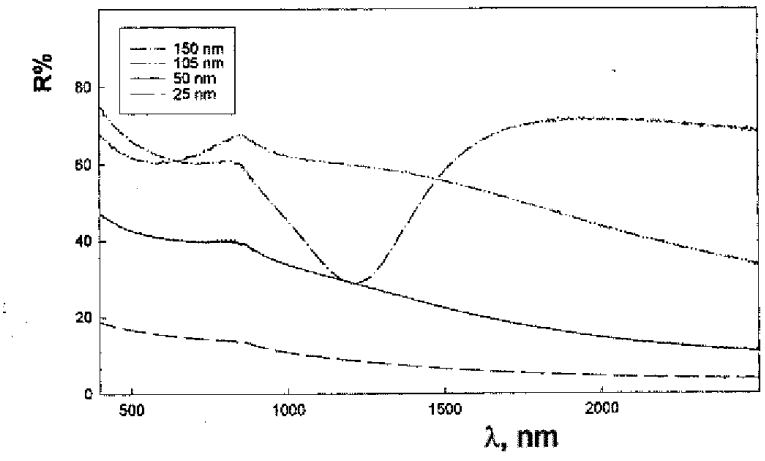

b

Fig. 4. Spectral distribution of a- transmittance T, b-reflectance R for $InSbTe_3$ thin films of different thicknesses in the (25-150) nm range.

3.3 Optical properties of InSbTe3 thin films

3.3.1 Spectral distribution of transmittance and reflectance

The spectral distribution values of transmittance T and reflectance R for $InSbTe_3$ thin films of different thicknesses, measured in (25-150) nm range are shown in Figs.4 (a) and (b). The

figures show that these films are transparent (T+R=1) in the wave length range (2100-2500) nm wavelength range. The spectral distribution of T and R for $InSbTe_3$ films measured in the (170-304) nm thickness range is shown in Figs.5 (a) and (b). From the figures it is observed that T+R<1 in the whole spectrum indicating that the films within this range of thickness posses absorption higher than the films in lower thicknesses (≤ 150nm). The reason of this behaviour may lie in true absorption (small deviations from stoichiometry and contamination), or scattering of light by surface and volume imperfections [25] (surface roughness, rough internal boundaries and density fluctuations, etc [25]). To clarify the main reason for the observed increase in absorption, optical microscope photographs, obtained for films of different thicknesses are represented in Fig.6. The presence of surface roughness for films of higher thicknesses (170-304nm) and homogeneity for thinner films (50nm) are indicated.

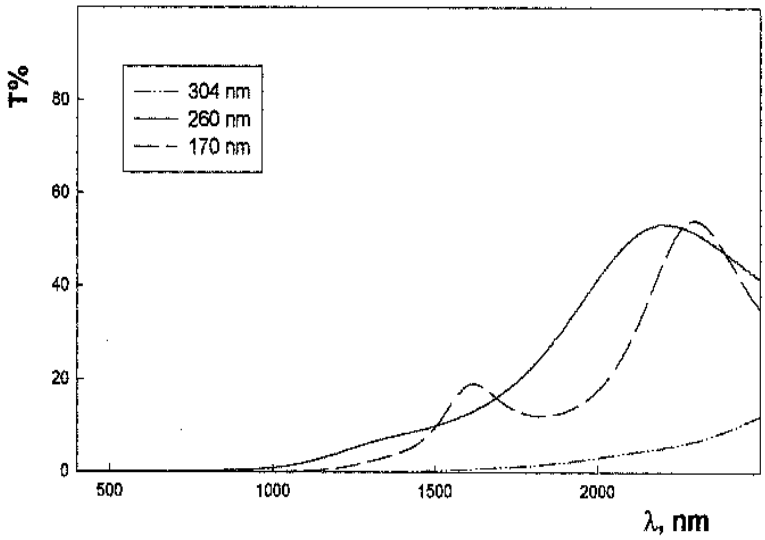

(a)

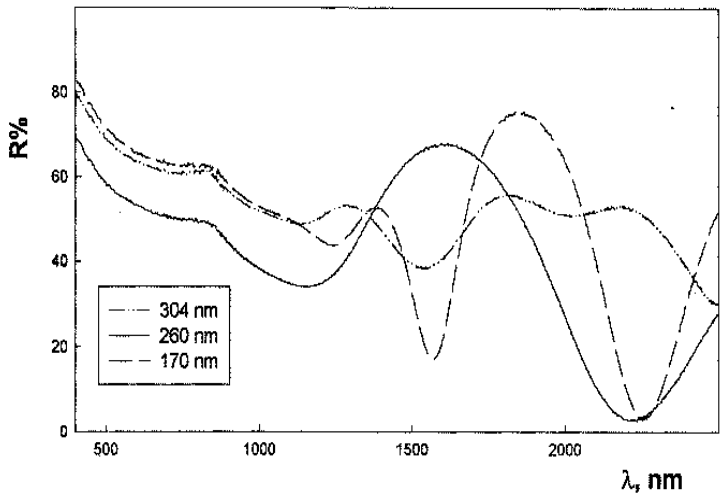

(b)

Fig. 5. Spectral distribution of a- transmittance T, b- reflectance R for $InSbTe_3$ thin films of different thicknesses in the (170-304) nm range.

3.3.2 Optical constants determination

Optical constants for $InSbTe_3$ films with thicknesses in the range (25-150) nm range are determined from measured transmittance and reflectance by solving Murmann's [26] exact equations using graphical method which involves considerable computations as follows. A reasonable range is chosen for *n* and *k* within which both refraction and absorption indices are simultaneously increased in steps of 0.1 and 0.05 respectively. Using Murmann's exact equations, a set of curves representing T and R as a function of d/λ (d is the film thickness) are drawn for different values of *n* at constant *k*. Using these standard figures and for every value of T and R at a given wavelength, a new curves of $[k=f(n)]_{n \text{ from } T}$ and $[k=f(n)]_{n \text{ from } R}$ are drawn. The point of intersection of each set of two new curves yields the required values of *n* and *k*. The same method was repeated over the whole spectral region and for other films of different thicknesses. Hence the dispersion curves for *n* and *k* were obtained and illustrated in Figs.7 & 8 respectively. It is indicated that the absorption index *k* is independent on film thickness in the considered range with an experimental error of ±2%, while the refractive index *n* decreases with increasing film thickness at any wavelength.

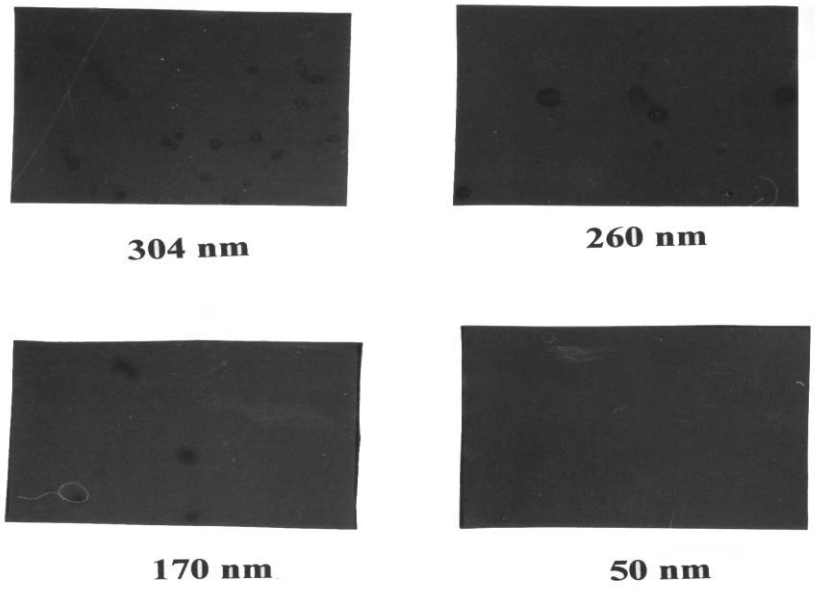

Fig. 6. Optical microscope of photograph for $InSbTe_3$ films of different thicknesses.

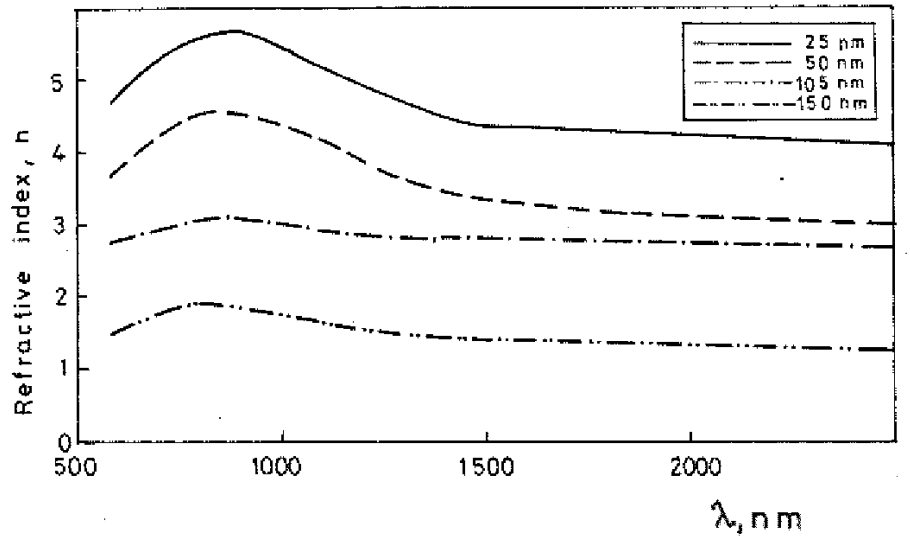

Fig. 7. Dispersion curves of refractive index n for $InSbTe_3$ films in the thickness (25-150) nm range.

3.3.3 Spectral distribution of the absorption coefficient α.

The absorption coefficient α of $InSbTe_3$ thin films is calculated using the well known equation ($\alpha = 4\pi k/\lambda$), in which *k* is the mean value of refractive index at each wavelength. The calculated values of α at different values of the wave length λ is represented as a function of the photon energy hυ and illustrated in Fig.9. It is clear from this figure that the spectral distribution can be divided into two regions:

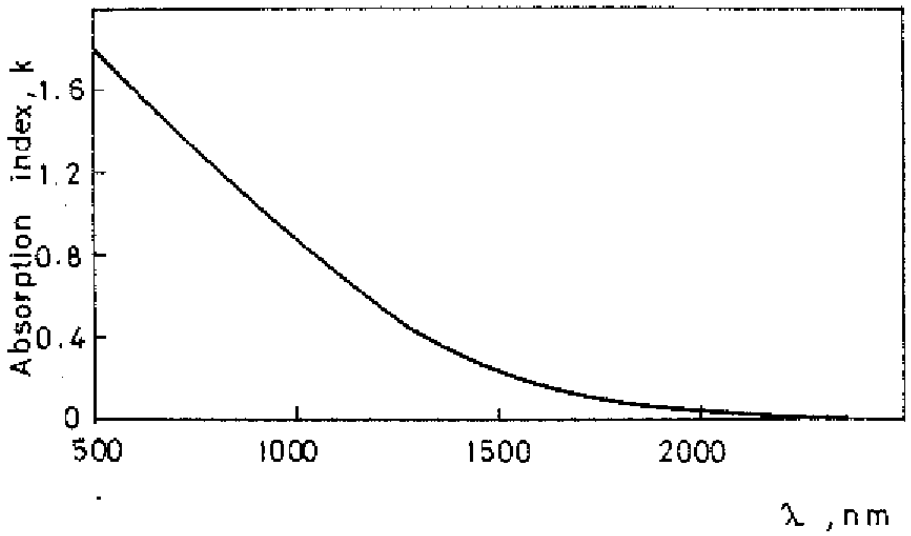

Fig. 8. Spectral distribution of absorption index k for $InSbTe_3$ in the thickness (25-150) nm range.

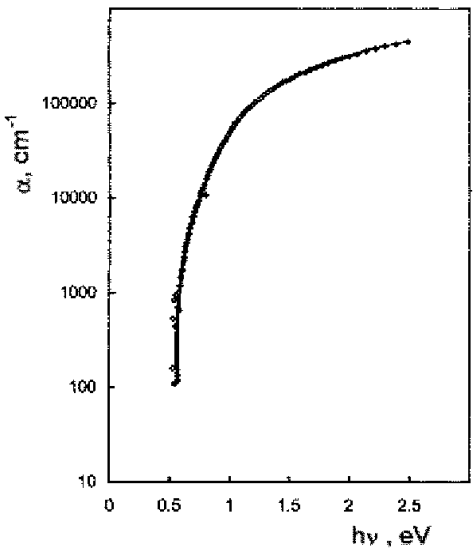

Fig. 9. Optical absorption coefficient α for $InSbTe_3$ thin films as a function of the photon energy $h\nu$.

(i) The exponential edge region where $\alpha(\nu)<10^4$ cm^{-1}, where the Urbach [27] tail appears. In this region the absorption coefficient is governed by the relation [27]

$$\alpha(\upsilon) = \alpha_o \exp\left(\frac{h\upsilon}{E_e}\right), \tag{3}$$

where E_e characterizes the band tail width. Therefore, plotting the dependence of log α as a function of hυ should give a straight line as in Fig.10 , from which both α_o and E_e can be evaluated (α_o = 0.01 cm^{-1} and E_e = 0.055 eV).

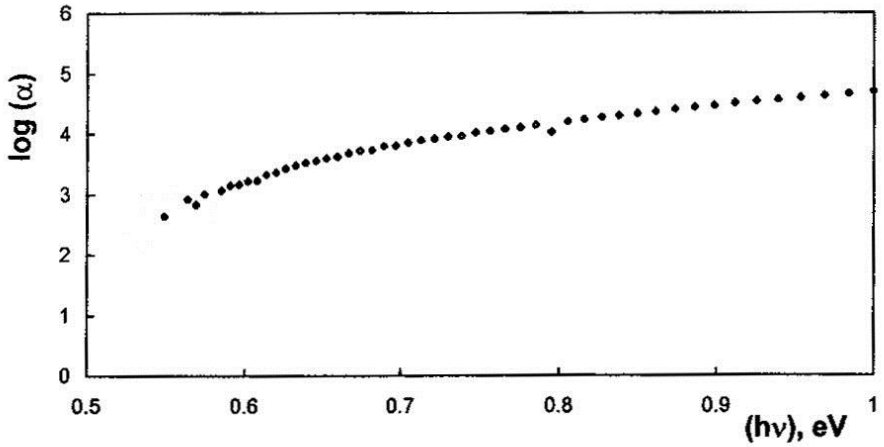

Fig. 10. Plots of log (α) as a function of $h\nu$ for $InSbTe_3$ thin films.

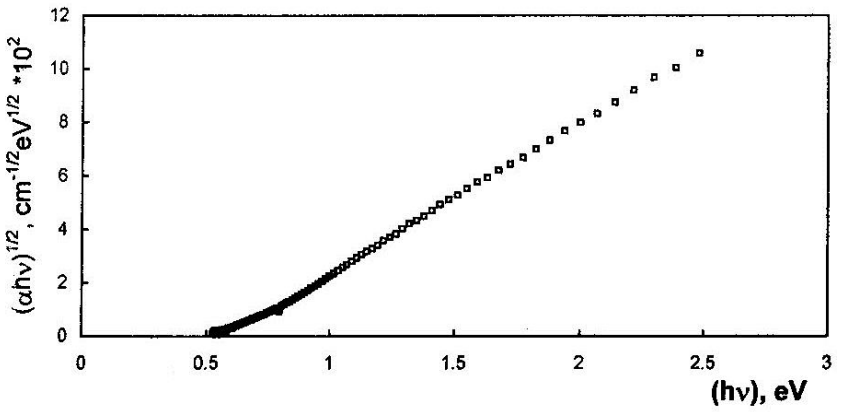

Fig. 11. Dependence of $(\alpha h\nu)^{1/2}$ on the photon energy $h\nu$ for $InSbTe_3$ thin films.

(ii) For higher values of $\alpha(\upsilon)>10^4$ cm^{-1}, the variation obeys the relation [22].

$$\alpha(\upsilon) = A\frac{\left(h\upsilon - E_g^{opt}\right)^r}{h\upsilon}, \text{ cm}^{-1} \qquad (4)$$

where A is a constant, E_g^{opt} is the optical energy gap of the material and r is the number which characterizes the transition process. In amorphous semiconductors, it takes the value of ½ and 2 for the direct and indirect allowed transitions respectively in amorphous semiconductors. Plotting $(\alpha\, h\upsilon)^{1/2}$ as a function of hυ as represented in Fig.11, shows a linear function indicating the existence of the indirect allowed transition. Extrapolation of the linear dependence of this relation yields the corresponding forbidden band width E_g^{opt}. The obtained value, of E_g^{opt} and the constant A (the slope of the linear part of this relation) from Fig.11 are 0.52 eV and $4.1\text{x}10^5$ cm^{-1} eV^{-1} respectively.

It is observed that the obtained value of E_g^{opt} (0.52 eV) lies between that of In_2Te_3 (1.01 or 1.025 eV) [28, 29] and that of Sb_2Te_3 (0.21 eV) [10].

4. Conclussion

The dc electrical conductivity of $InSbTe_3$ thin films increases with increasing both thickness in the range (25-150nm) and temperature in the range (303-393K). Temperature dependence of dc electrical conductivity of thin films of different thicknesses are nearly parallel lines in the considered ranges of thickness and temperature .This indicates that dc electrical activation energy ΔE_σ is single mean valued nearly independent on film thickness .Its mean value is 0.173 eV.

Optical constants *n* and *k* for $InSbTe_3$ amorphous thin films are determined from measurements of transmittance and reflectance in the wavelength range (400-2500nm). It is found that refractive index *n* decreases with increasing film thickness at any wave length, while absorption index *k* is practically independent on film thickness in the range (25-150nm). For films of thicknesses in the range (170-304nm), the spectral distribution of both T and R showed that T+R<1 in the whole spectrum. This is due to light scattering by surface roughness which is confirmed by electron microscope surface investigation. Analysis of the absorption index indicates

that the absorption mechanism refers to the existence of optical indirect transitions with optical gap of 0.52 eV. The width of the tails of the localized states in the gap region is 0.055eV.

References

[1] C. Julien, M. Eddrief, K. Kambas and M. Balkanski, Thin Solid Films **137**, 27 (1986).
[2] A. L. Zaslavskii, N. F. Kartenko, Z. A. Karachentseva, Sov Phys. Solid State **13**, 2152 (1972).
[3] G. L. Bleris, T. Karakostas, J. Stoemenos, N. A. Econonou, Phys. Status Solid A **34**, (1976) 243.
[4] M.A.M.Seyam, Applied Surface Science 181, 128 (2001).
[5] A. Zahab, M. Abd-Lefdil and M. Cadene, Phys. Status Solidi A 11.7 K 103 (1990).
[6] N. A. Hegaab, M. A. Afifi, A. E. El-Shazly and A. E. Bekheet, J. Mater. Sci. **33**, 2441 (1998).
[7] M. A. Afifi, E. Abd. El-Wahabb, A. E. Bekheet and H. E. Atyia, Acta Physica Polonica, **98**(40) 401 (2000).
[8] A.M.Farid, H.E.Atyia and N.A. Hegab, Vacuum, **80**, 284 (2005).
[9] M. Stordeur and G. Simon, Phys. Stat. Sol. (b) **124**, 799 (1984).
[10] R. Sehr and L. R. Testardi, J. Phys. Chem. Sol. **23**, 1219 (1962).
[11] J. Horak, K. Cermak and L.Koudelka, J. Phys. Chem. Sol. **42**, 805 (1986).
[12] J. Horak, Z. Stary, P. Lostak and J. Pancir, J. Phys. Chem. Sol. , **49**, 191 (1988)
[13] J. Kroutil, J. Navratil and P. Lostak, Phys. Stat. Sol. **131**, K 73 (1992).
[14] P. Lostak, R. Novatny, J. Kroutil and Z. Stary, Phys. Stat. Sol. (a) **104**, 841 (1987).
[15] V. A. Kulbachinskii, Z. M. Dashevskii, M. Inoue, M. Sasaki, H. Negishi, W. X. Gao, P. Lostak and J. Horak, Phys. Rev. B **52**(15) 10915 (1995).
[16] H.E.Atyia, A.M.A.El.Barry,Chalcogenide Letters **3**(5) 41 (2006).
[17] Liqiu Q.Men, Fusong S.Jiang, Chao Liu, Huiyong Liu,and Fuxi Gan, Proc. SPIE,Vol.2090, 82 (1996) ; doi : 10.1117/12.251980.
[18] J. Horak, S. Karamazov and P. Lostak, Phil. Mag. B **72**, 665 (1995).
[19] J. Horak, P. Lostak and L. L. Benes, Phil. Mag. B **50**, 665 (1984).
[20] M.A.M.Seyam, A.Elfalaky, Vacuum, **57**, 31 (2000).
[21] L.K.Chopra "Thin film phenomena " Printed in USA (1969)540.
[22] E.A.Davis and N.F.Mott, Phil. Mag., **22**, 903 (1970).
[23] H.Fritzsche and M. Kastner, Phil. Mag.B **37**, 285 (1978).
[24] N. F. Mott, Phil. Mag. **34**,1101 (1976).
[25] H. K. Pulker, appl. Opt. **18**, 1969 (1979).
[26] M. Murmann, Z. Phys. **80**, 161 (1933); Z. Phys., **101**, 643 (1936).
[27] F. Urbach, Phys. Rev. **92**, 1324 (1953).
[28] S. Sen and D. N. E. A. Davis and Bose, Solid State Comm. **50**, 39 (1984).
[29] G.Harbecke, G. Lautz, Z. Naturforsch **90**, 775 (1958).